doi:10.1016/j.jmb.2007.09.066 J. Mol. Biol. (2008) 375, 325–330

JMB

Available online at www.sciencedirect.com

ScienceDirect

ELSEVIER

COMMUNICATION

A Cytoskeletal Demolition Worker: Myosin II Acts as an Actin Depolymerization Agent

Lior Haviv, David Gillo, Frederic Backouche and Anne Bernheim-Groswasser*

Department of Chemical Engineering, Ben-Gurion University of the Negev, P.O. Box 653, Beer-Sheva 84105, Israel

Received 17 June 2007; received in revised form 24 September 2007; accepted 24 September 2007
Available online 29 September 2007

Myosin II motors play several important roles in a variety of cellular processes, some of which involve active assembly/disassembly of cytoskeletal substructures. Myosin II motors have been shown to function in actin bundle turnover in neuronal growth cones and in the recycling of actin filaments during cytokinesis. Close examination had shown an intimate relationship between myosin II motor adenosine triphosphatase activity and actin turnover rate. However, the direct implication of myosin II in actin turnover is still not understood. Herein, we show, using high-resolution cryo-transmission electron microscopy, that myosin II motors control the turnover of actin bundles in a concentration-dependent manner *in vitro*. We demonstrate that disassembly of actin bundles occurs through two main stages: the first stage involves unbundling into individual filaments, and the second involves their subsequent depolymerization. These evidence suggest that, in addition to their "classical" contractile abilities, myosin II motors may be directly implicated in active actin depolymerization. We believe that myosin II motors may function similarly *in vivo* (e.g., in the disassembly of the contractile ring by fine tuning the local concentration/activity of myosin II motors).

Keywords: actin bundle turnover; active filamentous actin depolymerization; blebbistatin; cryo-TEM; myosin II motors

Edited by J. Karn

Many processes in living cells are driven by molecular motors using ATP hydrolysis to generate work and motion.[1] Myosin II protein motors play key roles in a number of important processes,[2–8] some of which involve active assembly/disassembly of cytoskeletal substructures.[2,3,9–11] Close examination of the dynamics of certain cellular processes had revealed an intimate relationship between myosin II adenosine triphosphatase (ATPase) activity and actin turnover rate.[2,8,12–14] Myosin II motors function in actin bundle turnover in neuronal growth cones by promoting severing of the bundles into fragments that shrink over time[8] and in the recycling of actin filaments during cytokinesis.[12–14] The direct role of myosin II in the turnover of actin bundles has however not been elucidated, although it is believed to involve filament unbundling[15] and/or depolymerization.[8] Herein, we show that myosin II motors control actin bundle turnover in a concentration-dependent manner *in vitro*. We demonstrate that disassembly of actin bundles takes place in two stages—unbundling of the actin bundles into individual filaments and depolymerization of the filaments. We believe that myosin II motors may function similarly *in vivo* (e.g., in the disassembly of the contractile ring by tuning the local concentration/activity of the motors).

First, we studied the dynamics of the organization of actin/fascin bundles (AFBs) fluorescently labeled with Oregon Green® in the presence of myosin II motors in bulk. Figure 1 shows the final self-organization of this system after reaching a steady state. We were not able to observe the initial dynamics of our system owing to the limits of our

*Corresponding author. E-mail address: bernheim@bgu.ac.il.

Abbreviations used: AFB, actin/fascin bundle; ATPase, adenosine triphosphatase; cryo-TEM, cryo-transmission electron microscopy; Dabco, 1,4-diazabicyclo[2,2,2]octane; NEM-myosin II, *N*-ethylmaleimide myosin II.

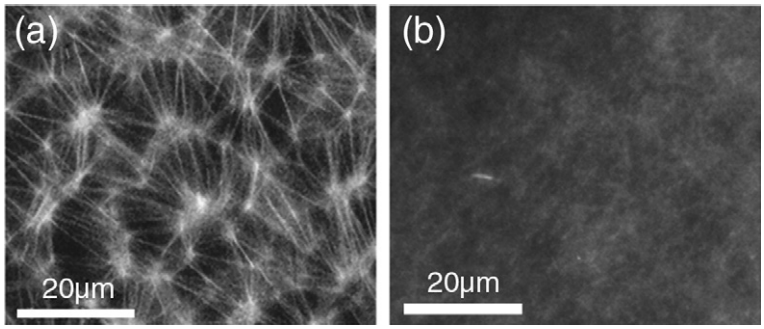

Fig. 1. Active self-organization of AFBs by myosin II motors. Fluorescence microscopy images were recorded at [A]=21 μM and [A]/[F]=10. (a) At a moderate concentration of myosin II, [A]/[M]=20, the motors reorganize actin bundles into dense triangular networks. (b) At an elevated motor concentration, [A]/[M]=2.9, myosin II inhibits formation and growth of AFBs; as a result, large-scale patterns cannot form. The polymerization buffer contains 10 mM Hepes, pH 7.6, 5.5 mM DTT, 0.12 mM 1,4-diazabicyclo[2,2,2]octane (Dabco), 0.133 M potassium chloride, 2 mM magnesium chloride, 1.7 mM magnesium–ATP, and an ATP-regenerating system composed of 0.1 mg/ml of creatine kinase and 1 mM creatine phosphate. Actin assembly was monitored by fluorescence microscopy with an Olympus 71X microscope (Olympus Co., Japan). Time-lapse images were acquired during 1–2 h with an Andor DV887 EMCCD camera (Andor Co., England). Data acquisition and analysis were performed with METAMORPH (Universal Imaging Co.). Actin was purified from rabbit skeletal muscle acetone powder.[23] Skeletal muscle myosin II was purified according to standard protocols.[24] Recombinant fascin, which was prepared with the use of a modification of the method of Ono *et al.*,[25] was expressed in *Escherichia coli* as a glutathione-*S*-transferase fusion protein. Actin was labeled on Cys374 with Alexa 568 or rhodamine (Cytoskeleton Inc.).

experimental setup, which allowed us to begin tracking only approximately 0.5 min after mixing. Addition of myosin II motors (at a ratio of [globular actin]/[myosin II]=[A]/[M]=20) at a moderate actin-to-fascin ratio ([globular actin]/[fascin]=[A]/[F]=10) induced the active organization of the AFBs into a dense triangular network (Fig. 1a). Surprisingly, a higher concentration of myosin II ([A]/[M]=2.9) totally prevented the formation of large structures, with only faint background fluorescence being visible in the optical micrograph (Fig. 1b). This faded fluorescence suggested that only individual actin filaments and/or actin monomers were present in the solution (which could not be optically resolved). At such a high motor concentration, the dynamics of the system appeared to be extremely rapid (<30 s; see above) and could not be temporally resolved. Our system did not further evolve to create large-scale structures; rather, it remained in an active steady state throughout the entire time span of the experiment (even after 2 h). In all the experiments, the ATP concentration was maintained at a constant millimolar concentration level by using an ATP-regenerating system. None of these phenomena occurred in the presence of inactivated *N*-ethylmaleimide (NEM) myosin II motors (which can only bind rigorously to actin filaments[16] and therefore do not generate forces and movements at the molecular level). This suggests that motor activity is essential for actin self-organization.

We recently showed that insight into the mechanism of the assembly/disassembly dynamics of AFBs may be provided by following the temporal evolution stages of a network of AFBs that self-organized at [A]/[F]=7 and [A]/[M]=10.[17] These concentrations were chosen with the aim of enhancing the effect of fascin, thus enabling the system to initially self-organize into a network but to disassemble over time owing to the activity of the motor molecules (see Fig. S1 in Ref. 17). After a few minutes, the network structure did indeed disentangle into long and straight individual AFBs (~30–40 μm). Under these conditions, the background of the optical image was blurred, indicating that both short actin filaments and/or very thin bundles (below optical resolution) and actin monomers were present in the solution. By the end of this process, the long AFBs had disappeared, leaving only short and thin actin filaments or bundles. Some agglomerations of actin were also observed.

To obtain a better understanding of the function of myosin II motors in the turnover of actin bundles and to reveal the processes occurring at the molecular level, we conducted high-resolution direct imaging by cryo-transmission electron microscopy (cryo-TEM). Comparisons of Fig. 2a, b, and c revealed that addition of myosin II motors to the medium produced a significant effect on bundle formation: in the absence of myosin II motors, straight and thick bundles were formed (Fig. 2a), whereas individual filaments were not observed. Addition of myosin II motors ([M]/[A]=0.1) to the solution resulted in thinner bundles, which could bend easily, and in individual filaments (Fig. 2b). Furthermore, addition of myosin II motors led to a decrease in the density of actin filaments/bundles vis-à-vis the myosin-free system (Fig. 2a). These findings imply a possible depolymerization of actin filaments/bundles, as manifested in the accumulation of actin monomers in the solution (small black dots as indicated by arrowheads in Fig. 2b, d, and e). At a higher content of motors, [M]/[A]=0.2, bundle formation was inhibited; the system was composed essentially of individual actin filaments, with a few loosely connected bundles (Fig. 2c).

In the presence of motors, we observed a variety of phenomena, including severing and splitting/opening of the bundles (Fig. 2d and e; compositions of actin, fascin, and myosin II in Fig. 2d and e are similar to those in Fig. 2b: [M]/[A]=0.1 and [F]/[A]=0.1). Severing of the bundles generated short fragments less than 1 μm in length (an example of such a bundle fragment is shown in Fig. 2d). In addition, splitting of bundle ends was frequently

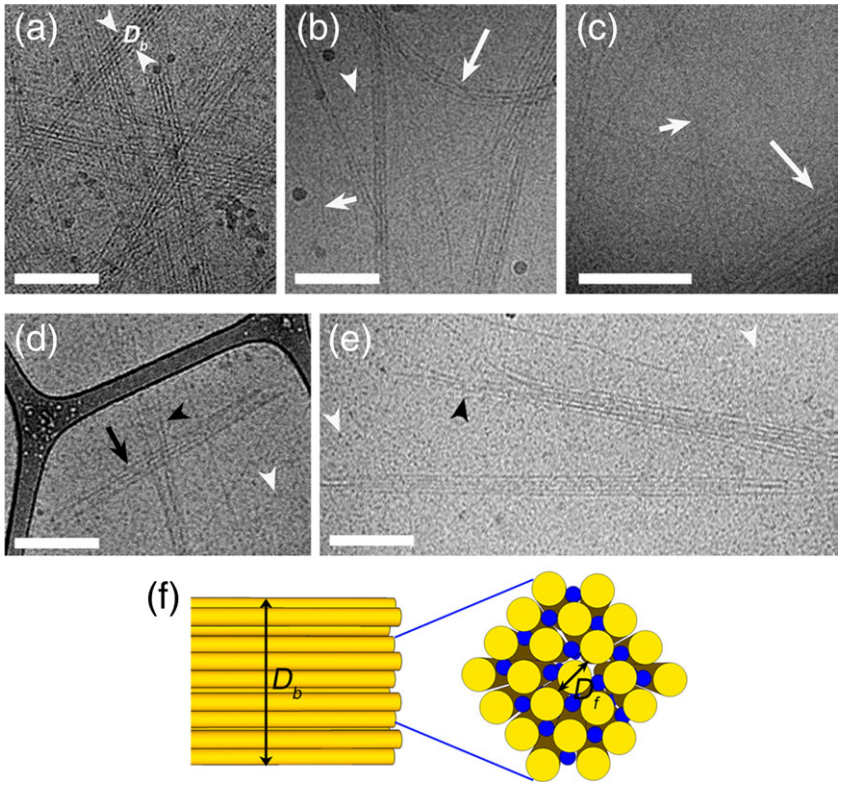

Fig. 2. High-resolution cryo-TEM imaging of actin bundle disassembly by myosin II motors. Micrographs were obtained at [A]=5 μM and [F]/[A]=0.1. (a) In the absence of myosin II motors, straight and thick bundles are formed; the two arrowheads indicate the diameter, D_b, of a bundle. No individual filament is evident. (b) At [M]/[A]=0.1, thinner bundles (long arrow), individual filaments (short arrow), and accumulation of actin monomers (small black dots as indicated by an arrowhead) are evident. (c) A high motor content, [M]/[A]=0.2, inhibits bundle formation. The system is composed essentially of individual actin filaments (short arrow); loosely connected bundles are seen but only rarely (long arrow). (d and e) A moderate myosin II concentration, [M]/[A]=0.1, can induce severing of bundles into short fragments (black arrow) or splitting (black arrowheads). White arrowheads indicate actin monomers. Bars represent 0.2 μm. (f) Schematic representation of a bundle. The bundle diameter is given by D_b (side view), and the area per filament in a bundle is given by D_f (top view; a blue ball represents a fascin protein, whereas a yellow circle represents an actin filament). After the individual components were mixed, the system was left to polymerize for 30 min at room temperature in polymerization buffer (10 mM Hepes, pH 7.6, 5.5 mM DTT, 0.12 mM Dabco, 0.133 M potassium chloride, 2 mM magnesium chloride, 1.7 mM magnesium–ATP, and an ATP-regenerating system composed of 0.1 mg/ml of creatine kinase and 1 mM creatine phosphate). We fixed the polymerization/bundling time at 30 min to ensure that the polymerization and bundling processes were completed. To confirm this assumption, we performed fluorescence microscopy measurements on the relevant solutions. Specimens for cryo-TEM were prepared in a controlled environment vitrification chamber.[26] All solutions were quenched from 25 °C and 100% relative humidity. A volume of 3 μl of the solution was carefully deposited on a TEM grid coated with holey carbon film (lacey carbon, 300 mesh grids, Ted Pella, Inc.). The grid was blotted with filter paper (Whatman no. 1) and plunged into liquid ethane at its freezing point. The vitrified samples were stored under liquid nitrogen before transfer to a TEM (Technai 12, FEI) operated at 120 kV with the use of a Gatan cryo-holder for imaging at −180 °C in low-dose mode and with underfocus at a few micrometers to increase phase contrast. Images were recorded on a multiscan CCD camera (Gatan 794 or Gatan 791) with the Digital Micrograph software package and analyzed by METAMORPH.

observed (Fig. 2d and e). Similar defects were also evident in the middle of bundles (data not shown).

The number of filaments per bundle, N_b, at different myosin II concentrations was determined from measurements of the bundle diameter, D_b, on the cryo-TEM images (Fig. 2). Considering a bundle as a cylinder or rod, we calculated the number of filaments, N_b, from the ratio A_b/A_f, where A_b is the cross-section area of the bundle, given by $A_b=(\pi/4)D_b^2$ (D_b is measured from the bundle's cross-section), and A_f is the effective cross-section area of an actin filament within the bundle, given by $A_f=(\pi/4)D_f^2$ (see Fig. 2f). The effective diameter, D_f, corresponds to the typical distance between two actin filaments in an AFB. In our calculation, D_f was kept constant at 9 nm.[15]

In Fig. 3a and b, we present the distribution of N_b obtained for the two systems shown in Fig. 2a and b, respectively. It is clearly evident that in both cases, with ([M]/[A]=0.1) and without ([M]/[A]=0) motors, the systems were highly polydispersed. The presence of the motors did not change the form of the distribution; both distributions fit an exponential decay function, $\mathrm{PDF}(N_b) \propto \exp(-N_b/N_{b,mean})$, where PDF is the probability distribution function and $N_{b,mean}$ is the mean number of filaments per bundle (the black lines in Fig. 3a and b mark the corresponding exponential fitting curves). The presence of the motors shifted the distribution to the left (i.e., to lower values of N_b). Figure 3c summarizes the mean bundle diameter, $D_{b,mean}$, and $N_{b,mean}$ values for the different myosin concentrations studied. The data show a monotonic decrease in both parameters with increasing motor concentrations. At the higher motor concentration of [M]/[A]=0.2 (system described in Fig. 2c), the solution contained mostly individual filaments or loose bundles. The values for $D_{b,mean}$ and $N_{b,mean}$ could therefore not be determined precisely and are not given.

The cryo-TEM experiments on AFBs showed that myosin II motors interfered with the bundling of

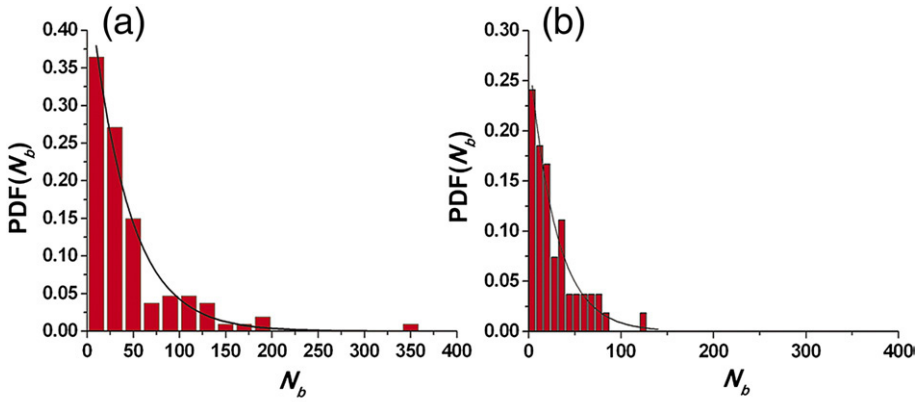

(c)

[Myosin II]/ [G-actin]	$D_{b,mean}$ [nm]	$N_{b,mean}$
0	52.2 ± 2.9	41.1 ± 3.0
0.05	48.1 ± 4.1	33.8 ± 6.3
0.1	43.4 ± 2.7	28.8 ± 2.5
0.2	Loose bundles	NA

Fig. 3. Quantitative analysis of the number of filaments per bundle, N_b, and AFB diameter, D_b, for [A] = 5 μm and [F]/[A] = 0.1. (a and b) Probability distribution functions (PDF) of N_b [PDF(N_b)] for [M]/[A] equal to 0 (a) and 0.1 (b). The black lines mark the corresponding exponential fitting curves. (c) Mean±SE values of diameters of the AFBs, $D_{b,mean}$, and number of filaments per bundle, $N_{b,mean}$, as a function of the [M]/[A] ratio.

actin filaments by fascin and induced severing and splitting of the bundles. These experiments also showed disassembly of actin in parallel with the unbundling process. The actin disassembly was manifested in a large decrease in the number of actin bundles and filaments and in an increase in the concentration of actin monomers in solution.

To study in greater detail the actin depolymerization process independently of the unbundling process, we conducted cryo-TEM experiments on

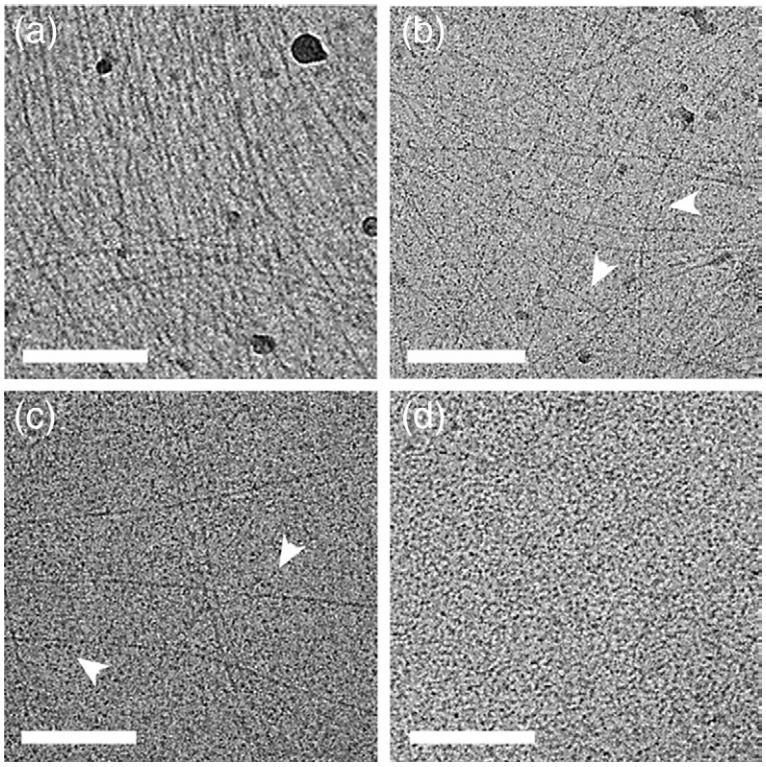

Fig. 4. Depolymerization of actin filaments by myosin II motors. Cryo-TEM micrographs were obtained at [A] = 2 μM and [M]/[A] equal to 0 (a), 0.1 (b), 0.5 (c), and 3 (d). (a) When no motor is added, an entangled network of actin filaments is observed. (b and c) Addition of myosin II motors induces a decrease in the concentration of filaments and an increase in actin monomers in the background (black dots in the background as indicated by arrowheads). (d) Eventually, at sufficiently high motor concentrations, no filament is observed; the system is composed solely of actin monomers. Bars represent 0.2 μm. These experiments were conducted in two stages: First, actin was polymerized without the addition of myosin II for 20 min. Then, myosin II motors were added, and the system was left to react for an additional 15 min. The polymerization buffer was composed of 10 mM Hepes, pH 7.6, 5.5 mM DTT, 8.8 mM Dabco, 0.133 M potassium chloride, 2 mM magnesium chloride, 1.6 mM magnesium–ATP, and an ATP-regenerating system composed of 0.1 mg/ml of creatine kinase and 1 mM creatine phosphate.

solutions of pure actin filaments in the presence of increasing amounts of myosin II motors (Fig. 4a–d). In the absence of myosin II motors, an entangled network of actin filaments was formed (Fig. 4a). Increasing the concentration of myosin II motors (Fig. 4b–d) induced a gradual decrease in the density of the actin filaments, up to their total disappearance above a certain content of motors (Fig. 4d). In parallel, the actin monomer concentration increased (Fig. 4c and d; seen as the density of black dots in the images' background). We can conclude from these qualitative findings that the concentration of filaments is reciprocally coupled to the monomer concentration, a conclusion that in turn may infer that the decrease in the filaments occurs as a result of depolymerization induced by the motor activity.

To confirm the correlation between motor ATPase activity and actin filament depolymerization, we conducted control cryo-TEM experiments in the presence of myosin II motors inactivated by either NEM or blebbistatin (Fig. 5). NEM-myosin II induces myosin–ADP rigor complexes, which bind tightly to actin filaments[16]; in contrast, myosin II ATPase inhibitors, such as blebbistatin, were reported to stabilize the myosin–ADP·Pi state, which binds actin filaments weakly.[18–20] The addition of these drugs did not inhibit the formation of myosin II minifilaments (such minifilaments are marked by white arrows in Fig. 5a). Rather, it generated a behavior that differed completely from that witnessed with active motors. In both cases, we observed that the density of actin filaments was remarkably higher than that in the presence of active motors (for comparison, see Fig. 4b, which represents an experiment carried out at the same actin and myosin II concentrations of 2 and 0.2 μM, respectively). Moreover, we observed the formation of large actin filament assemblies (bundles) (blebbistatin- and NEM-myosin II/actin systems in Fig. 5a and b, respectively) held together by the inactivated myosin II minifilaments (see the white arrows in Fig. 5a, which mark such blebbistatin myosin minifilaments connecting several actin filaments simultaneously). These findings were even more prominent when the concentration of inactivated motors was increased (data not shown).

In an *in vivo* study on the contractile ring, Wu and Pollard showed continuous disassembly of actin filaments, with a constant concentration of actin being maintained while the myosin II concentration increased locally.[3] This disassembly was coupled to the contraction of the contractile ring. In the current work, we showed qualitatively that actin bundle/filament disassembly was correlated to myosin II concentration. We can speculate that there is a similar correlation *in vivo*, which can infer on a control mechanism that is responsible for adjusting the actin disassembly during ring contraction. Similarly, a correlation between actin bundle turnover and myosin II activity in neuronal growth cones has also been proposed.[8]

In the current study, we showed that myosin II motors self-organized AFBs *in vitro* but only at moderate motor concentrations. At higher myosin II concentrations, the formation and growth of AFBs were dynamically inhibited. We also showed that the forces generated by the motors could induce, with time, disassembly of AFB networks into individual filaments and/or thin bundles. Our cryo-TEM experiments support these findings by showing in detail the origin of these processes at high resolution. We clearly demonstrated that myosin II motors disrupt bundle formation and induce severing and splitting of the bundles. Finally, herein we present additional evidence for the capacity of myosin II to induce the depolymerization of actin filaments *in vitro*.

The disassembly of actin bundles appears to take place in two consecutive steps: The first step is an unbundling process in which the actin bundles are disassembled into individual filaments. One possible explanation for this step is that the forces produced by the motors moving along actin filaments break the bonds between filamentous actin and fascin and therefore split the filaments (Fig. 2d and e). Another possible explanation lies in steric hindrance: minifilaments of myosin II, which are approximately 200–400 nm in length,[21] may sterically inhibit the binding of fascin. This phenomenon has recently been observed in a study on stress fibers showing that α-actinin and myosin II cannot be located at the same place along the fibers.[11] The

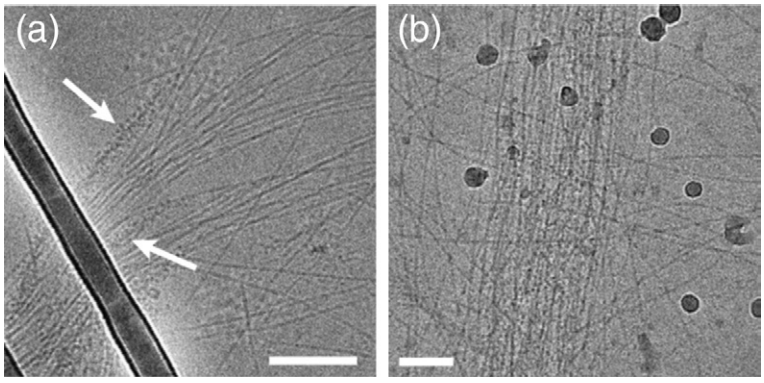

Fig. 5. Cryo-TEM images of actin filaments in the presence of inactivated myosin II motors. Conditions: [A]=2 μM and [M]/[A]=0.1. (a) Blebbistatin-myosin II/actin system. White arrows mark myosin II minifilaments attached to or embedded in the actin bundle. Bar represents 200 nm. (b) NEM-myosin II/actin system. Bar represents 100 nm. Both images show the formation of large actin bundles in the presence of minifilaments of the inactive motor. These motor aggregates act as passive cross-linkers, inducing the bundling of individual actin filaments and formation of large bundles.

second step in actin bundle disassembly is actin filament depolymerization (Fig. 4).

In vivo measurements of actin dynamics cannot discriminate between actin filaments and actin monomers. Herein, we show for the first time the direct relationship between myosin II activity and depolymerization of actin filaments in a concentration-dependent manner. To verify that these phenomena were directly associated with the activity of the motors, we used myosin II motors inactivated by NEM or blebbistatin, each of which inhibits the force-generating capabilities of the motors and therefore cannot produce work and movement at the molecular level but can only bind passively to actin filaments. In this case, none of the active phenomena described above was observed. Rather, large bundles of actin filaments were formed as a result of the cross-linking ability of the inactivated myosin heads.

Dynamic disassembly of filaments by motor proteins has been demonstrated for the MCAK kinesin motor, the first member of the family of microtubule-depolymerizing motors to be identified.[22] We suggest that, in addition to their "classical" contractile abilities, myosin II motors may be directly implicated in active actin depolymerization and actin filament turnover. Our results suggest that myosin II motors may function similarly *in vivo*. One possible mechanism for regulating actin disassembly/assembly dynamics in cells may be fine tuning the local concentration/activity of myosin II motors.

Acknowledgements

This work was supported by the Reimund Stadler Minerva Center for Mesoscale Macromolecular Engineering and by research grants from the Israel Cancer Association (ICA grant no. 20070020B) and Israel Science Foundation (ISF grant no. 551/04).

We thank Mr. Barak Gilboa and Ms. Inez Mureinik for their careful reading of the manuscript.

References

1. Howard, J. (1997). Molecular motors: structural adaptations to cellular functions. *Nature*, **389**, 561–567.
2. Pelham, R. J. & Chang, F. (2002). Actin dynamics in the contractile ring during cytokinesis in fission yeast. *Nature*, **419**, 82–86.
3. Wu, J.-Q. & Pollard, T. D. (2005). Counting cytokinesis proteins globally and locally in fission yeast. *Science*, **310**, 310–314.
4. Gallo, G., Yee, H. F., Jr & Letourneau, P. C. (2002). Actin turnover is required to prevent axon retraction driven by endogenous actomyosin contractility. *J. Cell Biol.* **158**, 1219–1228.
5. Ryu, J. *et al.* (2006). A critical role for myosin IIb in dendritic spine morphology and synaptic function. *Neuron*, **49**, 175–182.
6. Anderson, K. I., Wang, Y. L. & Small, J. V. (1996). Coordination of protrusion and translocation of the keratocyte involve rolling of the cell body. *J. Cell Biol.* **134**, 1209–1218.
7. Svitkina, T. M. *et al.* (2006). Analysis of the actin–myosin II system in fish epidermal keratocytes: mechanism of cell body translocation. *J. Cell Biol.* **139**, 397–415 (1997).
8. Medeiros, N. A., Burnette, D. T. & Forscher, P. (2006). Myosin II functions in actin-bundle turnover in neuronal growth cones. *Nat. Cell Biol.* **8**, 215–226.
9. Dean, S. O. *et al.* (2005). Distinct pathways control recruitment and maintenance of myosin II at the cleavage furrow during cytokinesis. *Proc. Natl. Acad. Sci. U.S.A.* **102**, 13473–13478.
10. Yamashiro-Matsumura, S. & Matsumura, F. (1986). Intracellular localization of the 55-kD actin-bundling protein in cultured cells: spatial relationships with actin, alpha-actinin, tropomyosin, and fimbrin. *J. Cell Biol.* **103**, 631–640.
11. Hotulainen, P. & Lappalainen, P. (2006). Stress fibers are generated by two distinct actin assembly mechanisms in motile cells. *J. Cell Biol.* **173**, 383–394.
12. Guha, M., Zhou, M. & Wang, Y. (2005). Cortical actin turnover during cytokinesis requires myosin II. *Curr. Biol.* **15**, 732–736.
13. Murthy, K. & Wadsworth, P. (2005). Myosin-II-dependent localization and dynamics of F-actin during cytokinesis. *Curr. Biol.* **15**, 724–731.
14. Burgess, D. R. (2005). Cytokinesis: new roles for myosin. *Curr. Biol.* **15**, R310–R311.
15. Ishikawa, R. *et al.* (2003). Polarized actin bundles formed by human fascin-1: their sliding and disassembly on myosin II and myosin V *in vitro*. *J. Neurochem.* **87**, 676–685.
16. Meeusen, R. L. & Cande, W. Z. (1979). *N*-Ethylmaleimide-modified heavy meromyosin. *J. Cell Biol.* **82**, 57–65.
17. Backouche, F. *et al.* (2006). Active gels: dynamics of patterning and self-organization. *Phys. Biol.* **3**, 264–272.
18. Limouze, J. *et al.* (2004). Specificity of blebbistatin, an inhibitor of myosin II. *J. Muscle Res. Cell Motil.* **25**, 337–341.
19. Kovács, M. *et al.* (2004). Mechanism of blebbistatin inhibition of myosin II. *J. Biol. Chem.* **279**, 35557–35563.
20. Allingham, J. S., Smith, R. & Rayment, I. (2005). The structural basis of blebbistatin inhibition in specificity of myosin II. *Nat. Struct. Mol. Biol.* **12**, 378–379.
21. Kaminer, B. & Bell, A. L. (1966). Myosin filamentogenesis: effects of pH and ionic concentration. *J. Mol. Biol.* **20**, 391–394.
22. Helenius, J. *et al.* (2006). The depolymerizing kinesin MCAK uses lattice diffusion to rapidly target microtubule ends. *Nature*, **441**, 115–119.
23. Spudich, J. A. & Watt, S. (1971). The regulation of rabbit skeletal muscle contraction: I. Biochemical studies of the interaction of the tropomyosin–troponin complex with actin and the proteolytic fragments of myosin. *J. Biol. Chem.* **246**, 4866–4871.
24. Margossian, S. S. & Lowey, S. (1982). Preparation of myosin and its subfragments from rabbit skeletal muscle. *Methods Enzymol.* **85**, 55–71.
25. Ono, S. *et al.* (1997). Identification of an actin binding region and a protein kinase C phosphorylation site on human fascin. *J. Biol. Chem.* **272**, 2527–2533.
26. Talmon, Y. (1999). In *Modern characterization methods of surfactant systems*, Marcel Dekker, New York.